PCAMM 2017 Poster Program

University of Victoria

December 9, 2017

University of Victoria | Centre for Advanced Materials & Related Technology

1. A Dynamic Impedance Study of the Initial Stages of Nickel Oxidation

M. Alikarami[1], T. Holm[1], D.A. Harrington[1,2,*]
[1]Centre for Advanced Materials and Related Technologies
[2]University of Victoria, Department of Chemistry
e-mail: dharr@uvic.ca

The nature of the species that form on oxidizing Ni electrode in alkaline solution has been studied for a long time. Bode summarized the formation and interconversion of these hydroxide and oxyhydroxide phases in terms of time and potential [1], but their structure and kinetics remain an active area of study [2]. The initially formed oxide is believed to be a hydrated hydroxide, α-$Ni(OH)_2$, which irreversibly interconverts to a less hydrated β-$Ni(OH)_2$ at higher potentials.

The formation and interconversion of these hydroxide phases is studied here by dynamic electrochemical impedance spectroscopy (dEIS) [3,4], which applies a multi-frequency waveform during a cyclic voltammetry sweep or during a chronoamperometry experiment. It enables the study of non-steady states of the surface that cannot be accessed by conventional potentiostatic EIS. It is particularly suited to study the irreversible α-$Ni(OH)_2$ to β-$Ni(OH)_2$ interconversion.

An electrochemical polishing procedure was used to remove the oxide layer in order to have a clean and oxide-free surface before doing the experiment. This step consisted of galvanostatic holding in phosphoric acid solution. Impedance data were collected during voltammograms at different slow sweep rates, with selected hold periods before, during, or after the peaks, and were correlated to charges under the voltammograms. The impedance data were fitted to equivalent circuits. In most cases the faradaic impedance approximated a charge-transfer resistance, but the use of complex capacitance plots showed evidence for additional structure at low frequencies. Comparison of the polarization resistance determined from the slope of the voltammograms with the estimated low-frequency intercept of the impedance showed a discrepancy in the peak region, which also suggests that a slow process exists that whose kinetics is not determinable by dEIS.

The sweep-hold experiments followed the conversion of the α phase to the β phase, and found that the oxidation is not complete in the potential range of 0.2-0.3 V. Voltammograms of the admittance at selected frequencies were found to be sensitive to the surface condition, and showed that the surface condition did not return to the same value after cycling.

This research was conducted as part of the Engineered Nickel Catalysts for Electrochemical Clean Energy project administered from Queen's University and supported by Grant No. RGPNM 477963-2015 under the Natural Sciences and Engineering Research Council of Canada (NSERC) Discovery Frontiers Program.

References

[1] H. Bode, K. Dehmelt and J. Witte. *Electrochim. Acta.*, **11**, 8 (1966).
[2] M. Alsabet, M. Grden and G. Jerkiewicz, *Electrocatalysis*, **2**, 4 (2011).
[3] R.L. Sacci, F. Seland and D.A. Harrington, *Electrochim. Acta.*, **131**, 13 (2014).
[4] R.L. Sacci and D.A. Harrington, *ECS Transactions*, **19,** 31 (2009).

2. Plasmonic Light–Trapping in Next–Generation Photovoltaic Cells

B. Brady[1], V. Steenhoff[2], M. Vehse[2], A. G. Brolo[1]

[1]Centre for Advanced Materials and Related Technologies, University of Victoria, Canada
[2]DLR Institute of Networked Energy Systems, Oldenburg 26129, Germany
e-mail: bbrady@uvic.ca

1st generation solar cells dominate the solar panel market and make up the majority of the solar panels seen on rooftops and in solar farms around the world. These solar cells are fabricated from high-purity crystalline silicon wafers which are expensive and highly energy-intensive to manufacture. Thin-film photovoltaics, or 2nd generation solar cells, are of great interest due to decreased manufacturing costs, improved environmental sustainability and the potential for flexible, semi-transparent, and light-weight modules. Unfortunately, most thin-film solar cell types have limited power conversion efficiency due to poor optical absorption. The scientific literature thus contains a plethora of work incorporating wavelength-scale nanostructures within thin-film solar cells to increase optical absorption by focusing light within solar cell absorbing layers. With next-generation transition metal dichalcogenide monolayer solar cells on the horizon, the ability to focus light into ultra-thin layers is of upmost interest.

In this work, nanostructured ultra-thin-film solar cells are designed to incorporate various effects to trap-light within the absorbing layer. Fig. 1 shows the solar cell design concept with schematics of the light-trapping mechanisms: (1) optical cavity standing wave resonances, (2) optical waveguide mode excitation coupled through diffraction from the NP array, and (3) near-field plasmonic enhancements of metallic NP arrays. Fabricated nanostructured solar cells showed significant performance enhancements compared reference solar cells, as shown on the right in Fig. 1. By a direct comparison of Ag and SiO_2 NP arrays, we were able to clearly show a plasmonic contribution to current generation, as shown in the simulated field profiles on the left of Fig. 1. To our best knowledge, such an unambiguous demonstration of plasmonic enhancement has yet to be presented for in the literature for inorganic solar cells. The concepts demonstrated in this work can be directly translated to next-generation photovoltaic devices.

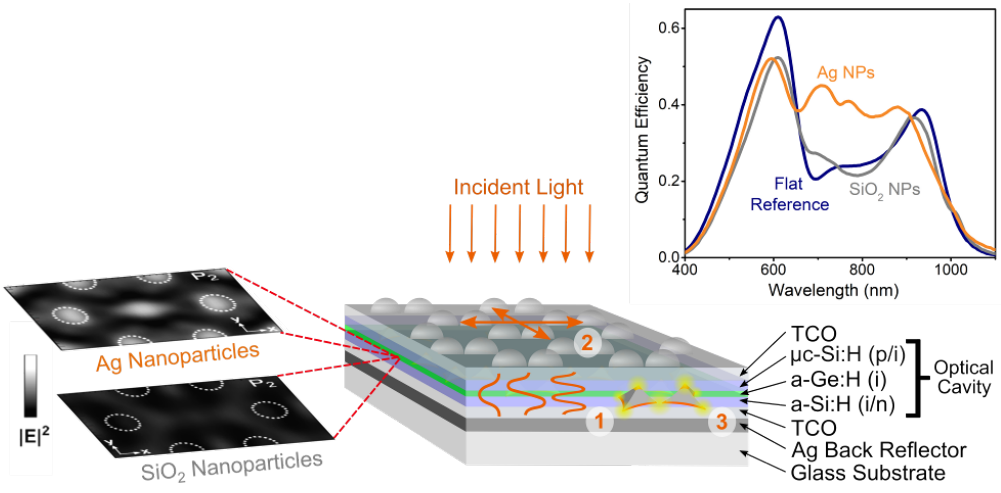

Fig. 1 Ultra-thin-film solar cell designed to incorporate 3 distinct optical enhancement mechanisms by nanostructuring with plasmonic nanoparticle arrays. Quantum efficiency curves on the right show significant performance enhancements for structured cells relative to flat reference cells. Simulations on the left show a plasmonic enhancement effect.

This work was supported by NSERC CREATE and the exchange program IPID4all - Mobile Doctorates in System Integration of Renewable Energy, which is funded by the DAAD (German Academic Exchange Service).

3. Evolutions of Chemical and Polar Structures and Properties in the Lead-Barium Zirconate Titanate (BPZT) System

X. Wang[1], H. Wu[1,2], A. A. Bokov[1], Z.-G. Ye[1]
[1]Simon Fraser University, Department of Chemistry and 4D LABS
[2]Donghua University, Department of Applied Physics
e-mail: zye@sfu.ca

Relaxor ferroelectrics are a class of disordered crystals possessing peculiar structure and properties. $(Ba_{1-x}Pb_x)(Zr_{0.30}Ti_{0.70})O_3$ (BPZT) shows relaxor behavior due to the BZT relaxor portion of the solid solution. It is interested that the interaction of the $6s^2$ lone pair electrons from the Pb may have on this relaxor behavior. In order to study the evolution of polar structure and chemical structure (compositional order-disorder) in materials, the BPZT solid solution was synthesized with the Ba^{2+} gradually replaced by Pb^{2+}.

The characterization of crystal structure, dielectric behavior and ferroelectric properties of the material with various compositions was analyzed through XRD, dielectric spectroscopy and ferroelectric measurement. Unexpectedly, a non-monotonic variation of the relaxor behavior was found during the substitution of Pb^{2+} for Ba^{2+}. When x=0.1, BPZT solid solution exhibits a most evident relaxor behavior with a lowest T_{max}. This increase is due to the increased amount of disordered states in polar nanoregions (PNRs). However, with the further increase of the Pb concentration, long range order begins to reform again and thus decreasing relaxor behavior.

Additional interest comes from the crossover from relaxors to ferroelectrics, including the phase transition from cubic to tetragonal and the PNRs to FE domains. When $0.4 < x < 0.5$, BPZT solid solution shows a dielectric anomaly, the frequency dependence of the anomaly exhibits dielectric relaxation following the Vogel–Fulcher law, indicating relaxor-like behavior. The relaxor state in the BPZT solid solution occurs after the ferroelectric phase transition upon cooling, indicating a re-entrant phenomenon.

References

[1] G. H. Haertling, *J. Am. Ceram. Soc.*, **82**, 797 (1999).
[2] A. A. BOKOV and Z.-G. YE, *J.Matter. Sci.*, **41**, 32 (2006).
[3] N. Zhang, Z. Xu, Y. Feng, *Journal of Electroceramics,* **21(1-4)**, 609–612 (2007).
[4] C. Lei., Ph.D. Theses., Simon Fraser University (2008).

4. A new device to evaluate Radiotherapy response of tumor cells

A. Palacios[1,2], S. Harder[3], P. Meksiarun[4], A. G. Brolo[1,2*],
[1]University of Victoria, Department of Chemistry
[2]Centre for Advanced Materials and Related Technologies
[3]University of Victoria, Department of Physics and Astronomy
[4]University of British Columbia Okanagan, Department of Physics
E-mail: americap@uvic.ca

Raman spectroscopy is an increasingly widespread laser based method for characterizing biological species. Although the Raman scattering signals are relatively weak, it provides several advantages over different laser techniques. For example, prior sample manipulation is not required, this is particularly useful for in-vivo cell assays to which addition of metal components, for signal enhancement, or incorporation of fluorescence biomarkers, could produce stress driven chemical or physical composition changes.

It has been proven the capabilities of a Raman spectroscopy approach for monitoring radiation-induced biochemical responses occurred during radiotherapy [1]. In this studies, human cell lines (H460, MCF7, and LNCaP) were radiated with relevant doses of radiation (1-10 Gy) and changes on Raman spectra were analyzed at post-radiated times. The intracellular glycogen content was used as a biomarker for radiosensitivity correlation[2].

Coupling this studies to microfluidics could improve the current spectral acquisition protocol and lead to the automation of the process. For this purpose a new device suitable for use in research and clinical laboratories, capable of flowing, analyzing and recovering live cells, as well as decreasing experimental times and sample consumption, needs to be fabricated.

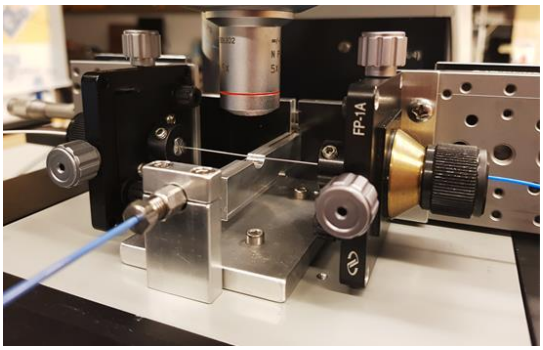

Fig. 1. Microscope setup component

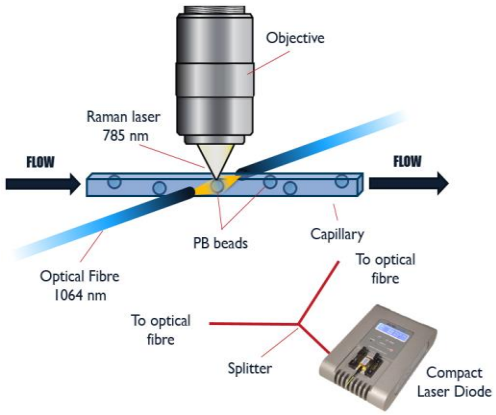

Fig. 2. Fused silica capillary as preliminary microfluidics system for cell flowing.

Especial acknowledgement to BC Cancer Agency Vancouver Island Centre

References

[1] S. Harder, M. Isabelle, AG. Brolo, J. Lum and A. Jirasek, *Scientific Reports* **6**, Article number: 21006 (2016)
[2] Q. Matthews, M. Isabelle, S. Harder, J. Smazynski, W. Beckham, AG. Brolo, et al., *PLoS ONE* **10,** e0135356 (2015)

5. Highly Sensitive Vanadium Pentoxide Thin Films For Directional Room Temperature IR Sensing

Siamack V. Grayli[⊥],Gary W. Leach[∥] and Behraad Bahreyni[⊥]

[∥] Department of Chemistry,Simon Fraser University, CANADA
[⊥] Integrated Multi-Transducer Systems Laboratory (IMuTS Lab), Simon Fraser University, CANADA
e-mail: svgrayli@sfu.ca

Vanadium pentoxide thin films have been deposited on quartz substrate via organic sol-gel synthesis and dip coating. The process was developed to establish a reliable and inexpensive method to produce thin films with high temperature coefficient of resistance for sensing applications. The resulting thin films were placed into two groups based on the alkoxide precursor concentration used to synthesize the sol from vanadium oxy-tri-isopropoxide as the precursor alkoxide, isopropanol as the solvent and glacial acetic acid. Quartz substrates were then coated with the sol and annealed under different conditions. Effects of changes in the precursor concentration in the synthesized sol, different degrees of crystallinity of the post-annealing thin films, and stoichiometry of the deposited thin films were studied via morphological and structural analyses. The temperature coefficient of resistance values for these thin films lied in the range of -3%K-1 to -4%K-1, comparing favorably to films produced through existing techniques such as DC magnetron sputtering, chemical vapor deposition or pulsed laser deposition.

We are also reporting on use of vanadium pentoxide as a thermos-resistive sensing layer on a patented vector light sensor design whereby the changes in the material's electrical resistance as result of radiative heat absorption and in conjunction with the sensor's three dimensional topology, allows for the detection of both the distance between the sensing pixels and the radiation source and the angle of incidence. The main application foreseen for the vector light sensor is room temperature proximity detection to allow real-time directional infrared sensing in manufacturing facilities co-occupied by human work force and industrial robotic arms.

Selected References

[1] H. A. Basantani et al., "Enhanced electrical and noise properties of nanocomposite vanadium oxide thin films by reactive pulsed-dc magnetron sputtering," Appl. Phys. Lett., vol. 100, no. 26, p. 262108, 2012.
[2] P. Wang et al., "High Sensitivity 17 μ m Pixel Pitch 640 ×512 Uncooled Infrared Focal Plane Arrays Based on Amorphous Vanadium Oxide Thin Films," IEEE Electron Device Lett., vol. 36, no. 9, pp. 923–925, Sep. 2015.
[3] S. S. N. Bharadwaja et al., "Processing issues in pulse DC sputtering of vanadium oxide thin films for uncooled infrared detectors," Adv. Electroceramic Mater. II Vol. 221, pp. 177–185, 2010.
[4] M. S. de Castro, C. L. Ferreira, and R. R. de Avillez, "Vanadium oxide thin films produced by magnetron sputtering from a V 2 O 5 target at room temperature," Infrared Phys. Technol., vol. 60, pp. 103–107, 2013.
[5] C. Venkatasubramanian, O. M. Cabarcos, D. L. Allara, M. W. Horn, and S. Ashok, "Correlation of temperature response and structure of annealed VO x thin films for IR detector applications," J. Vac. Sci. Technol. Vac. Surf. Films, vol. 27, no. 4, pp. 956–961, 2009.
[6] P. Guggilla, A. K. Batra, J. R. Currie, M. D. Aggarwal, M. A. Alim, and R. B. Lal, "Pyroelectric ceramics for infrared detection applications," Mater. Lett., vol. 60, no. 16, pp. 1937–1942, 2006.

6. In-situ X-ray Diffraction of Fuel Cell Catalyst Layers

I. Martens[1], J. Drnec[2], D.P. Wilkinson[1], D. Bizzotto[1]
[1]University of British Columbia, Clean Energy Research Centre
[2]European Synchrotron Radiation Facility
e-mail: imartens@chem.ubc.ca

The commercialization of proton exchange membrane (PEM) fuel cells has increasingly demanded lower precious metal catalyst loadings. A better understanding of platinum nanoparticle degradation mechanisms and electrochemistry will be essential in preserving fuel cell performance over increased device lifetimes. In-situ synchrotron x-ray diffraction/scattering is a powerful tool for characterizing commercial catalyst layers in an electrochemical cell[1-2]. Recent advances in hardware presently allow time-resolved scattering measurements and diffractive imaging[3] without compromising electrochemical experiments. New cell designs[4] greatly improve the ease and flexibility of measuring membrane electrode assemblies under environmental conditions and Pt loadings relevant for fuel cell operation and degradation.

The structural effects and kinetics of platinum electrochemistry on nanoparticles can be directly probed using x-ray diffraction. The evolution of nanoparticle strain, atomic ordering, oxidation, and dissolution are monitored in the presence of adsorbing molecular species under potential control. We show how by monitoring Pt particle size, and Pt lattice strain, it is possible to deconvolute chemical and electrochemical steps in the mechanism of Pt oxidation and reduction.

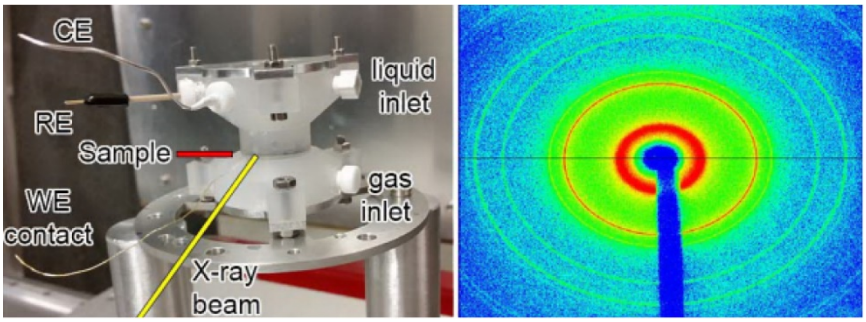

Figure 1. X-ray transparent half-cell suitable for high-energy x-ray diffraction of membrane electrode assemblies (left). X-ray powder diffractogram obtained from fuel cell cathode during oxygen reduction reaction (right).

References

[1] H. Imai, K. Izumi, M. Matsumoto, Y. Kubo, K. Kato and Y. Imai. *J. Am. Chem*. Soc., **131** (17), 6293–6300,(2009)
[2] K. Sasaki, N. Marinkovic, H.S. Isaacs, and R.R. Adzic. ACS Catal., **6** (1), pp 69–76 (2017)
[3] F. Reikowski, T. Wiegmann, J. Stettner, J. Drnec, V. Honkimaki, F. Maroun, P. Allongue, O.M. Magnussen. *J. Phys. Chem. Lett.*, **8** (5), pp 1067–1071 (2017)
[4] B. Pinaud, A. Bonakdarpour, L. Daniel, J. Sharman and D.P. Wilkinson. *J. Electrochem. Soc.*, **164** (4),ppF321-F327,(2017)

7. Magnetic and Structural Properties of Novel Fe(II) and Fe(III) Complexes Using Mossbauer Spectroscopy

Leah Gajecki[1*], Barbara D. Sawicka[2], David J. Berg[1]

[1]University of Victoria, Department of Chemistry
[2]University of Victoria, Department of Mechanical Engineering
e-mail: lgajecki@uvic.ca

Novel Fe(II) and Fe(III) complexes have been synthesized using a carbazole based di-tetrazole ligand (iPr4N). The structure of these complexes has been determined by the use of Mossbauer spectroscopy when X-Ray crystal structures were unattainable. The magnetism of these complexes has also been followed using Mossbauer spectroscopy, along with solid state magnetometry and solution magnetic data. The most interesting of these complexes is a bis-ligand Fe(II) complex ($(iPr4N)_2Fe$) that shows a thermally induced spin crossover (SCO) transition, from low spin (LS) at low temperatures to high spin (HS) at high temperatures. This spin transition is clearly seen through the solid state magnetic data as well as the Mossbauer data. An interesting two-step transition can be seen in the solid state magnetic data where around room temperature there is a spin-admixed system where a portion of the Fe centers are low spin and a portion are high spin; this is rarely seen in SCO complexes. The Mossbauer spectrum measured at room temperature (RT) shows a mix of 38% LS and 62% HS Fe(II) present, consistent with the magnetic data. The SCO complexes showing the inherent bistability (HS and LS) are interesting as they may be useful as molecular switches or information storage devices[1]. The magnetic properties of this compound and other Fe compounds will be presented.

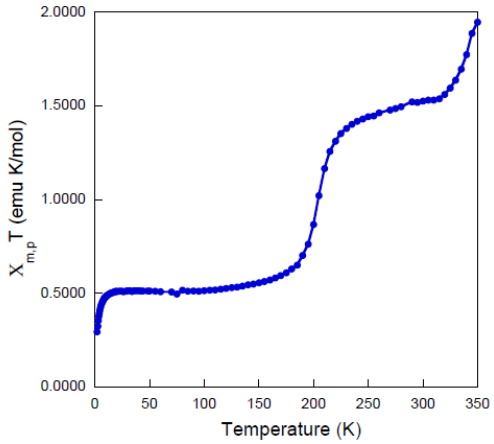

Figure 1. Solid state magnetic data of $(iPr4N)_2Fe$

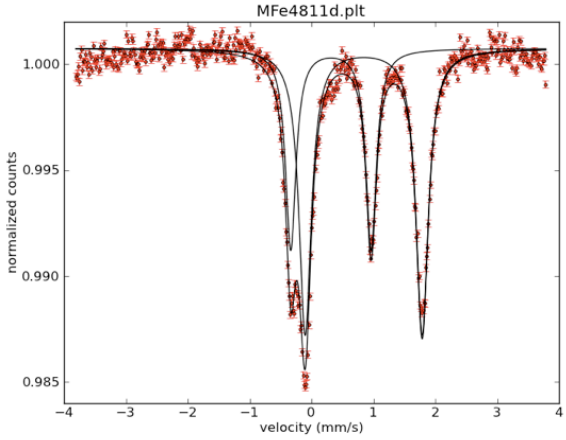

Figure 2. RT Mossbauer spectrum of $(iPr4N)_2Fe$

1. Gamez, P.; Costa, J. S.; Quesada, M.; Aromi, G., Iron Spin-Crossover compounds: from fundamental studies to practical applications. *Dalton Transactions* **2009,** (38), 7845-7853.

8. Incorporation of metal nanoparticles into polymer delivery vehicles for combined photo-ablation and chemotherapy

Sundiata Kly, Sarah Eaton, Matthew Moffitt*, Devika Chithrani**

University of Victoria

skly@uvic.ca

Modern chemotherapy research is broadening passed traditional drug molecule screening and clinical application. It seems as though the era of non-supra-molecular designer drugs has reached maximum efficacy. The dose related toxicity is a result of the failure of these simple systems to differentiate between healthy and cancerous cells. In the end nanotechnology will be embraced to fulfill the shortcomings of traditional medicine. The inability to address the heterogeneity of the tumour environment is still a barrier for nanomedicine beyond the regular barriers that effect any medication. To deal with the heterogeneity of the tumour environment multifunctional metal nanoparticle polymer assemblies containing the anti-cancer drug paclitaxel have been made. [1] Each portion of the assembly, the metal, the polymer, and the paclitaxel play a role in the efficacy of the combined photo-ablation chemotherapy treatment.

Metal nanoparticles are key in creating precision in photo-ablation therapy, because they are used to create the heat in areas where they are located like cancer cells in a tumor. [1] The uptake of metal nanoparticles into cells is largely size dependent. Smaller nanoparticles under 20 nm are desirable for photo-ablation because of their increased surface area, but have lower cellular uptake. [2] Presented here is a method to increase the cellular uptake of smaller gold nanoparticles while adding the functionality of a chemotherapy drug to penetrate further into the tumor. Moreover we are able to demonstrate control of the morphology through microfluidic processing without changing chemical parameters. [3] The metal nanoparticle assisted photo-ablation can only happen where the nanoparticles can reach. The dense nature of tumor stroma and the heterogeneity of the vasculature often create regions inaccessible to nanoparticles. [1] The EPR effect should allow for accumulation of polymer delivery vehicles in regions adjacent to inaccessible regions. Here the secondary function of metal nanoparticles releases paclitaxel to diffuse to regions the metal nanoparticles cannot access. [1] The combined effect should provide increased efficacy of treatment.

This work was supported by NSerc grant # 157819

References

[1] C. Yang, J. Uertz, and D. Chithrani, *Nanomaterials*, **6(48)**, 1-15 (2016).

[2] D. Chithrani, A. Ghazani, C. Chan, *Nano Lett*, **6**, 662-668 (2006).

[3] A. Bains, Y. Cao, S. Kly, J. Wulff, and M. Moffitt, *Molec. Pharm*, **14**, 2595-2606 (2017)

9. Tailoring the DNA SAM surface density on different surface crystallographic features using potential assisted thiol exchange

K. K. Leung[1,2], A. D. Gaxiola[1,2], H.-Z. Yu[3], D. Bizzotto[1,2,*]
[1]Advanced Materials and Process Engineering Laboratory
[2]University of British Columbia, Department of Chemistry
[3]Simon Fraser University, Department of Chemistry
e-mail: bizzotto@chem.ubc.ca

Formation of alkyl thiol self assembled monolayers (SAMs) using potential-assisted deposition has been shown to be an efficient way of forming SAMs with less defects. [1,2] Using this method to control DNA surface coverage on a DNA SAM would have many applications for manufacturing portable diagnostic biosensor-type devices. A method of forming DNA alkyl thiol self-assembled monolayers on gold using potential-assisted thiol exchange is examined using direct imaging methods. This was done using an initial mercaptohexanol self assembled monolayer initially formed on a gold monocrystalline bead, followed by deposition of fluorophore labelled thiol modified DNA while applying a potential (Fig. 1). A gold monocrystalline bead electrode enables analysis on the effect of surface crystallography or surface atomic structure on the SAM formation using electrochemical fluorescence microscopy imaging to directly image DNA surface coverages.

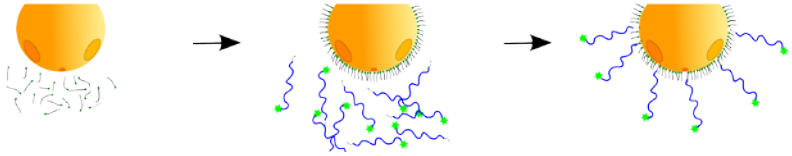

Fig. 1 A MCH layer is assembled on a monocrystalline Au bead then DNA is deposited into the MCH layer at a constant potential (E_{app})

Applying positive potentials result in a 10x higher DNA coverage compared to when no potential was applied (Figure 2). Low index crystallographic facets (111,100, 110) after an hour have similar DNA coverage while high index features (210 and 311) features having the lowest and highest amounts of DNA. Applying negative potentials also result in a higher but less uniform DNA layers with only the 111 facet and surrounding facets having higher DNA coverage. The effect of electrolyte composition also appears to have an effect with chloride ions facilitating the potential-assisted thiol exchange at positive potentials. Detailed evaluation of the DNA SAMs will be further discussed.

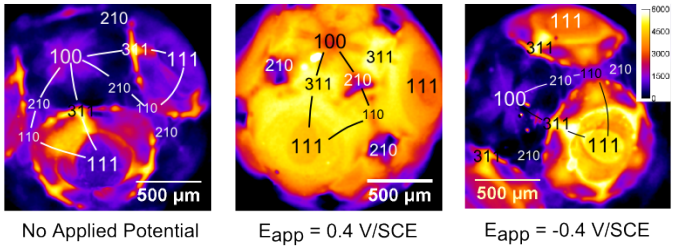

Fig. 2 Fluorescence Images taken of DNA SAMs made with potential-assisted thiol exchange at varying E_{app}

This work was supported by NSERC (Canada) Discovery and Equipment Grants and Mitacs Globalink

References

[1] F. Ma and R. B. Lennox, *Langmuir*, **16**(15), 6188 (2000).
[2] D. A. G. M. Jambrec, F. La Mantia and W. Schuhmann, *Angewandte Chemie*, **54**, 15064 (2015).
[3] Z. L. Yu, J. Casanova-Moreno, I. Guryanov, F. Maran and D. Bizzotto, *Journal of American Chemistry Society*, **137**, 276 (2015).

10. In situ analysis of organic NLO crystal growth

S. Roy[1], D. Hore[1,*]
[1]University of Victoria, Department of Chemistry
e-mail: dkhore@uvic.ca

Most common nonlinear optical (NLO) crystals used today are inorganic based, such as β-barium borate and $AgGaS_2$. Even though inorganic NLO crystals are more readily available and have higher damage thresholds, organic NLO crystals have been shown to be promising for nonlinear applications because of their faster optical response, higher bandwidth and stronger nonlinear response. Multiple amino acids crystallize in non-centrosymmetric space groups. This has been linked to the strong intermolecular hydrogen bonding network they form. One study has shown that histidine crystals have strong nonlinear properties [1]. Since then, studies have been done on crystals of L-histidine and histidine derivatives to assess their nonlinear properties. L-histidine has also been shown to crystallize in different forms depending on the solvent it is in. In water, an orthorhombic structure is observed, while in ethanol, histidine crystallizes in a monoclinic form. This highlights the importance to study crystal growth in situ as its environment can drastically change its properties.

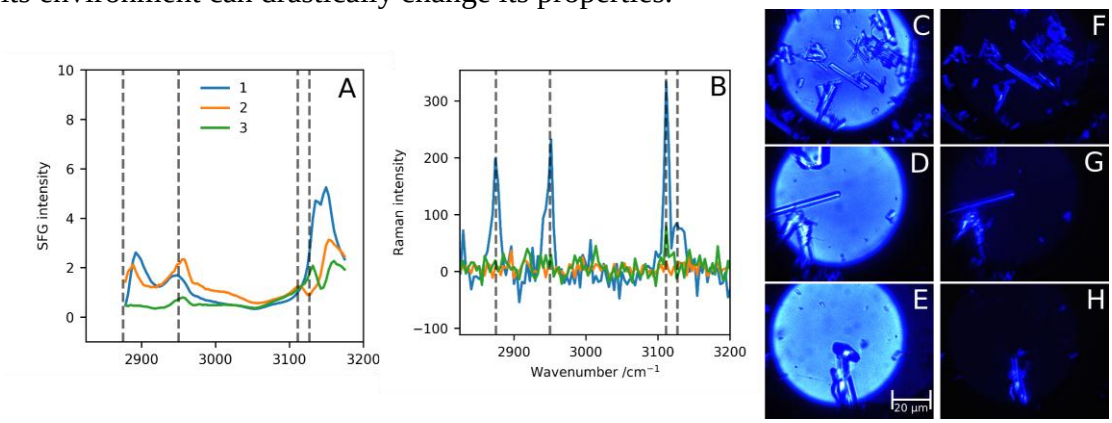

Fig. 1. SFG (A) and Raman (B) spectra of crystals probed in situ with their respective bright field images (1: C, 2: D, 3: E) and cross polarized images (1: F, 2: G, 3: H)

To study the crystal growth in situ, crystals have to be isolated and analyzed separately. A way to do so is to study them when they are adsorbed on a surface. The use of bright field imaging on the surface can then be used to allow for visualization of the crystals presence, size and shape. A new instrumental set up was constructed to allow for multiple techniques to probe the same area. Broadband SFG, polarized TIRR, bright field imaging and polarized imaging were used to measure the vibrational response and the orientation dependence of L-histidine crystals in situ. The results showed a strong correlation between the crystal orientation at the surface and the spectroscopic response for both SFG and TIRR. Since the TIRR signal can't be negative but the SFG showed negative contribution to the nonlinear susceptibility in certain orientations, polarized TIRR could be used as a probe of the overall crystal alignment within the plane of the surface, while SFG can assess the degree of orientation in a specific direction.

References

[1] G. I. Dovbeshko, L. I. Berezhinsky and V. V. Obukhovsky, *Proc. SPIE*, **2795**, 306 (1996).

11. Photoelastic Modulator-Based Broadband Mid-Infrared Stokes Polarimeter

William R. FitzGerald[1], Dennis K. Hore*[1]
[1]University of Victoria, Department of Chemistry
e-mail: williamf@uvic.ca

The Stokes vector is a four-element vector which completely describes the polarization state of light. A Stokes polarimeter is an instrument capable of measuring the Stokes vector, and thereby the polarization state. Presently, designs for Stokes polarimeters are abundant for wavelength regions outside of the infrared [1-4], where they are mainly used for astronomical applications. Designs in the mid-infrared are relatively scarce due to a paucity of suitable materials, but can be especially useful for materials analysis given the chemical and structural information contained within the vibrational modes of a material [5]. The design, calibration, and operation of a novel dual photoelastic modulator-based Fourier transform broadband Stokes polarimeter was accomplished. This instrument measures the full Stokes vector in the 2.5-11~μm range in the mid-infrared. The FTIR source produces a broadband beam of light, which travels through several polarization-state modulating optics, which build polarization information into the signal at the detector. As the FTIR steps through hundreds of mirror positions, the signal from the detector is demodulated at four frequencies, creating four interferograms. These interferograms are Fourier transformed to produce intensity spectra for each of the four Fourier coefficients of interest.

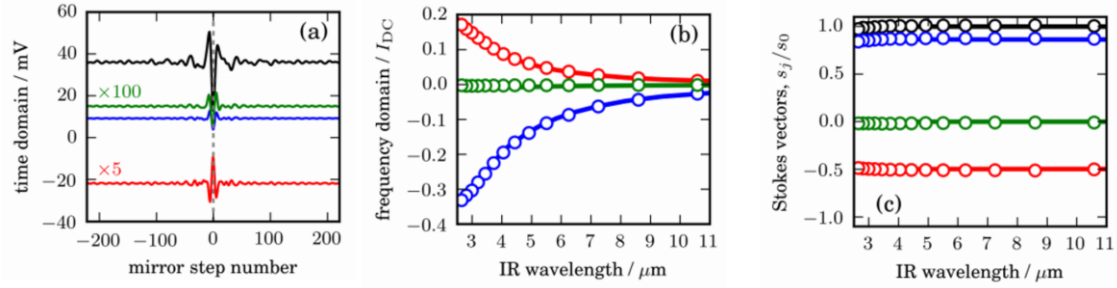

Fig. 1 – Data collection and transformation to Stokes vectors for 60° linearly polarized light.

The derivation of analytical expressions to produce the Stokes vector from the intensity spectra is quite simple at a single wavelength, as PEMs can be calibrated specifically to reduce mathematical complexity. These simplifications cannot be done in a multi-wavelength scheme given that the properties of the PEMs are wavelength dependent, and the full analytical expressions are quite complicated. For materials characterization, the light from the source is typically polarized prior to being transmitted through a sample. The polarimeter then measures the resulting polarization state. This scheme has been applied to the measurement of the electro-optic properties of cadmium zinc telluride (CZT) crystals, as well as refractive index measurements of a quartz waveplate. These experiments demonstrate the applicability of this instrument to materials investigations.

References

[1] F. Schäfers, H.C. Mertins, A. Gaupp, W. Gudat, M. Mertin, I. Packe, F. Schmolla, S.D. Fonzo, G. Soullíe, W. Jark, *Appl. Opt.*, **38**, 4074–4088 (1999).
[2] T. Koide, T. Shidara, M. Yuri, N. Kandaka, H. Fukutani, K. Yamaguchi. *Rev. Sci. Instrum.*, **63**, 1458–1461 (1992).
[3] K.J. Voss, Y. Liu., *Appl. Opt.*, **36**, 6083–6094 (1997).
[4] T. Hofmann, V. Gottschalch, M. Schubert, *Appl. Phys. Lett*, **91**, 121908 (2007).
[5] A. Röseler, *Infrared spectroscopic ellipsometry*; Wiley-VCH Verlag GmbH, Weinheim (1990).

12. Low Temperature Photoluminescence Studies of $Hg_3Se_2I_2$ Single Crystals

Shaun Cooke,[1*] Svetlana Kostina,[1] Yihui He,[2] Mercouri Kanatzidis,[2] Bruce Wessels,[3] Thomas Tiedje[1]

[1] *Department of Electrical and Computer Engineering, University of Victoria, BC, V8P 5C2, Canada*
[2] *Department of Chemistry, Northwestern University, Evanston, IL, 60208, USA*
[3] *Department of Materials Science and Engineering, Northwestern University, Evanston, Illinois 60208, United States*
*e-mail: scooke23@uvic.ca

Suitable semiconductors for X- and gamma ray detectors operable at room temperature are in demand as current materials used have high cost and inevitable growth issues. $Hg_3Se_2I_2$ crystals were gown using vapor transport with dimensions 5x5x0.1 mm^3 [2]. High Z metals like mercury and iodine provide good stopping power for high-energy photons. Therefore the compound $Hg_3Se_2I_2$ that has a band gap of 2.15 eV is an attractive material for X-ray detectors [1]. The large band gap allows the device to operate at higher temperatures and voltages than materials with lower band gaps. $Hg_3Se_2I_2$ is also attractive as an X-ray detector because of its desirable optical and electrical properties [2].

Photoluminescence (PL) spectroscopy is a non-invasive technique to measure quality of semiconductor materials. PL measurements on $Hg_3Se_2I_2$ reported previously showed five overlapping peaks in the visible range between 1.4 eV and 2.3 eV at T=15 K [2]. Four of these peaks are considered to be donor-acceptor pair recombination while the other is attributed to excitons. However, no observations of deep levels using PL in the IR range for h_ν<1.4 eV have been reported up to now. In this work, PL measurements were performed on a $Hg_3Se_2I_2$ single crystal using a 532 nm 5 mW pump laser and a liquid nitrogen cooled InGaAs array detector sensitive in the 0.8 eV to 1.8 eV range. The PL spectrum at T=9 K revealed two peaks centered at 1.12 eV and 1.43 eV. The dependence of PL emission intensity with incident laser power indicated that both peaks are due to donor-acceptor pair recombination. Temperature dependence was also investigated between T = 9 K and 110 K. Results indicate that the peak centered at 1.12 eV experienced a blue shift with no change in the full width at half maximum (FWHM) while the 1.43 eV peak underwent a blue shift and then a subsequent redshift with increasing FWHM. Activation energies determined from the temperature dependence of PL will be discussed and compared to the activation energies determined by thermally stimulated current spectroscopy and temperature dependence of dark current [1].

[1] Kim, J., Peters, J., He, Y., Liu, Z., Das, S., Kontsevoi, O., Kanatzidis, M. and Wessels, B. (2017). *Physical Review B*, 96
[2] He, Y., Kontsevoi, O., Stoumpos, C., Trimarchi, G., Islam, S., Liu, Z., Kostina, S., Das, S., Kim, J., Lin, W., Wessels, B. and Kanatzidis, M. (2017). *Journal of the American Chemical Society*, 139, pp.7939-7951.

13. High Temperature Electrooxidation of Glycerol on Nickel

Tory Borsboom[1,2], Thomas Holm[1], Han Bao[1], David A. Harrington[1,2]
[1]Centre for Advanced Materials and Related Technologies
[2]University of Victoria, Department of Chemistry
e-mail: borsboomtory@gmail.com

Long term glycerol electro-oxidation product selectivity is greatly affected by the temperature the experiment is run at. This has been shown via HPLC using an Aminex HPX-87H column. Experiments are typically done over the course of 48 hours using a custom autoclave setup originally created by Thomas Holm [1,2]. A standard three electrode electrochemical cell is setup inside the autoclave, with separation between working, reference, and counter electrodes.

Using standard calibration curves in the HPLC we are able to quantitatively determine the amount of each product formed, as well as their identity. In room temperature experiments we show that Formic Acid dominates the product selectivity, but at higher temperatures we see a shift towards more complex acids such as Glyceric and Glycolic Acid. Additionally, at 80 °C we see the formation of a new product that we have yet to identify.

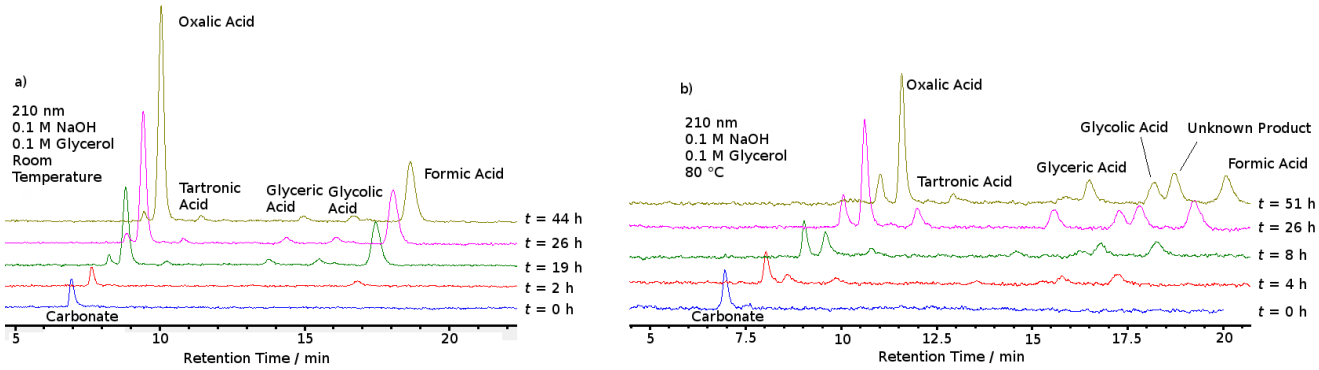

Fig. 1. a)HPLC results from a long term glycerol electro-oxidation at room temperature. b) HPLC results from a long term glycerol electro-oxidation at 80 °C.

This research was conducted as part of the Engineered Nickel Catalysts for Electrochemical Clean Energy project administered from Queen's University and supported by Grant No. RGPNM 477963-2015 under the Natural Sciences and Engineering Research Council of Canada (NSERC) Discovery Frontiers Program.

References

[1] T. Holm, P.K. Dahlstrøm, S. Sunde, D. A. Harrington, F. Seland, *ECS Trans*, **75**, 1055, (2016).
[2] T. Holm, P.K. Dahlstrøm, O.S. Burheim, S. Sunde, D.A. Harrington, and F. Seland, *Electrochim. Acta.*, **222,** 1792 (2016).

14. Fabrication, Characterization and Spectral Simulation of GaAs/GaAsBi Solar Cell

M. Mahtab[1], Z. Jiang[2], V. Bahrami-Yekta[1], T. Tiedje[1], R. Lewis[3], M. Masnadi Shirazi[4]
[1] Electrical Engineering Department, University of Victoria, BC, Canada
[2] Electrical Engineering Department, Simon Fraser University, BC, Canada
[3] Paul-Drude-Institut für Festkörperelektronik, Hausvogteiplatz 5-7, Berlin, 10117, Germany
[4] Electrical Engineering Department, University of British Columbia, BC, Canada
e-mail: m.mahtab.83@gmail.com

Epitaxial n+/p and p+/n junction diodes of GaAs/GaAsBi structure were grown on doped GaAs. The same steuctures without Bi incorporation was grown as reference. Thickness of the layers, doping concentration and the Bi content of the structures were determined by the growth rate, beam equivalent pressure and substrate temperature. Target growth condition for desired doping concentration was done by sets of calibration samples and investigation of grown epi-layer structures was done by high-resolution x-ray diffraction (HRXRD) as a post growth characterization. The gold contacts of 10 nm were evaporated by electron beam at low pressure on either side of the samples.

The photovoltaic (PV) performance of devices, was done by 150 W Xenon lamp (Newport Co.), passing through a AM1.5G filter at room temperature to find out the current–voltage (I–V) characteristics of the fabricated solar cells. Solar response has been simulated using continuity equations under low-injection condition [1] in an abrupt p/n junction to find out the minority carrirs diffusion currents as well as drift current contribution of the depletion region to the total current density and external quantum efficiency has been calculate.

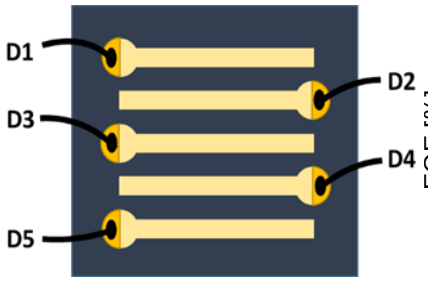

Fig 1: top: The top view of contact evaporation and wiring for solar performance measurement

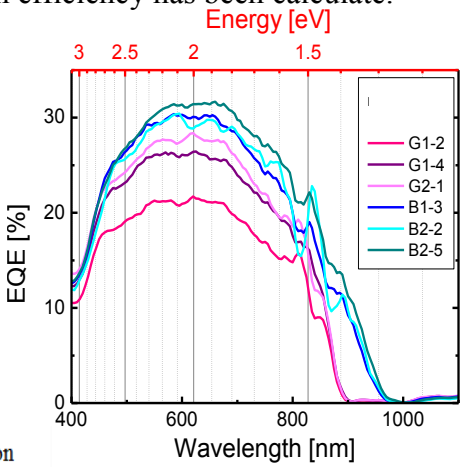

Fig2: Spectral response of n+/p device.

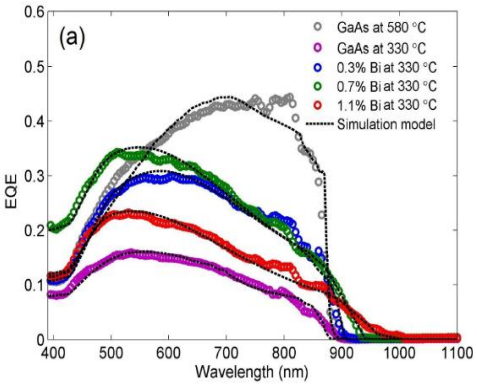

Fig3: Spectral response of p+/n device.

As we can see in Figure 1and 2, with introduction of Bi into GaAs, a non-zero EQE below the GaAs band edge is obtained, indicating that the photon absorption and carrier generation have taken place in GaAsBi alloys at longer wavelengths than that in GaAs which confirms that GaAsBi alloys extend the photovoltaic operation of solar cells to longer wavelengths.

References

]1[S. M. Sze and K. K. Ng, Physics of semiconductor devices. John Wiley & Sons., 2006.

15. Probing Discotic Liquid Crystalline Dimer Self-assembly

C.Zellman[1], V. Williams[1*]

[1]Simon Fraser University, Department of Chemistry and 4D LABS, Burnaby, BC, V5A 1S6

Canada

,

e-mail: czellman@sfu.ca

Disc-shaped (discotic) liquid crystals (DLCs) have garnered attention for their potential application as organic semiconductors in organic light-emitting diodes (OLEDs), photovoltaics, and field-effect transistors[1]. DLC dimers are an attractive class of organic materials for their ability to form glassy liquid crystal (LC) phases, which allows liquid crystalline ordering to be locked, even under conditions in which the LC phase is not thermodynamically favoured[2]. A major challenge pertaining the DLC dimer field is correlating molecular conformation to liquid crystalline self-assembly, and this continues to hinder the DLC field given its electronic properties greatly depend on the LC self-assembly[3,4]. My research focuses on the design of DLC dimers, with an emphasis on understanding how molecular structure alters the conformational dynamics of these systems and their self-assembly.

Molecular conformation appears to strongly dictate self-assembly of discotic dimers, and determining molecular conformation becomes exceedingly difficult with discotic dimers that can fold. In a discotic dimer two aromatic cores ("discs") are bound to a flexible linker, which enables the molecule to fold via intra-molecular π-π interactions between the discs. This folding effect can be probed using ^{1}H-NMR, as a significant upfield shift in the aromatic region is observed in the dimer with respect to the monomer when the dimer is folded. Given that folding determines the overall molecular conformation, controlling folding is vital to control liquid crystalline self-assembly. In my work, I've systematically investigated a group of dimers in which the stereochemistry and flexibility of the linker have been manipulated. Analysis of their folding behaviour and liquid crystalline self-assembly using various techniques have revealed that the folding and self-assembly are very sensitive to the stereochemistry and flexibility of the linker. My work provides important insight into how folding affects molecular conformation, and in turn liquid crystalline self-assembly. Further studies may provide new techniques for controlling liquid crystalline self-assembly through control of molecular conformation, which would enable better design of DLC dimer materials.

References

[1] Goodby, J. W. *et al*. Raynes, P. *Handbook of Liquid Crystals (Volume 1)*, Wiley-VCH: Weinheim, **2014**.

[2] Kumar, S. *Chemistry of Discotic Liquid Crystals from Monomers to Polymers*, CRC Press - Taylor & Francis Group: Boca Raton, **2011**.

[3] Sutton, C. *et al*. *Chem. Mater.*, **2016**, *28*, 3-16.

[4] Thorley, K. J. *et al*. *Chem. Mater.*, **2017**, *29*, 250-2512.

16. Dual Function PD-L1-seeking Gold Nanoparticles: Functionalisation and Characterisation

D. Blevins[1], K. Bromma[2], B. D. Chithrani[2], J. E. Wulff[1]
[1]University of Victoria, Department of Chemistry
[2]University of Victoria, Department of Physics and Astronomy
e-mail: djblevin@uvic.ca

The PD-1/PD-L1 interaction is one of great interest to immunology and oncology. The receptor (PD-1) and ligand (PD-L1) are pivotal proteins for checks necessary in the prevention of autoimmune responses [1]. T-cells will screen for PD-L1, if this fails, cytotoxic T-cells will proliferate in that area. However, cancers overexpress PD-L1 yielding a similar outcome, this false positive allows tumours to remain undetected. Blocking PD-L1 on tumours will allow for an immune response to occur within the tumour microenvironment, suppressing growth [2]. Overexpression of PD-L1 is a character biomarker in tumour recognition and protein of interest in cancer research [3]. Clinical cases show that antibodies and small molecule inhibitors for PD-L1 are capable of suppressing this "invisibility" in a variety of tumours by simple blockading [4,5].

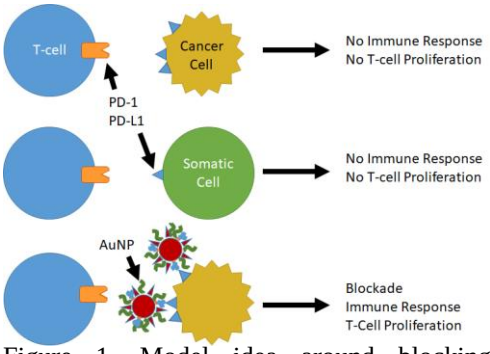

Figure 1. Model idea around blocking PD-1/PD-L1 interaction with functionalised gold nanoparticles (AuNPs).

Alongside inhibition of protein-protein interactions, cancers are treated by radiation therapy which may cause vicinal cells to become oncogenic [6]. Cancer treatments have taken steps in the use of gold nanoparticles (AuNPs) [7] as they can be used as radiation dose enhancers. By functionalising AuNPs to target PD-L1, it may be possible to suppress tumour growth and decrease collateral tissue damage in radiation-based therapies. The goal of this project is to characterise small molecules and functionalise them onto AuNPs. Surface plasmon resonance (SPR) is a characterization tool, to measure interactivity between PD-1, PD-L1, small molecules, and the AuNPs. An antibody for PD-L1 has been characterised and optimized for the conjugation to AuNPs. The antiPD-L1 was optimized for synthesis by conjugating the antibody to sufficient oxidized glutathione (GSSG) via EDC coupling, which was then purified by spin column centrifugation and reduced 5 molar equivalents of TCEP. The thiol-mAb was then mixed with RGD peptide and PEG2000 (15:300:600) onto bare AuNPs. SPR displayed that these AuNPs were binding to PD-L1 5-fold greater than free antiPD-L1.

This work was supported by NSERC, the University of Victoria, the Michael Smith Foundation for Health Research, and the Canada Chairs Program.

References

[1] Sharpe, A. H., Wherry, E. J., Ahmed, R., and Freeman, G. J. *Nat. Immunol.* **8**, 239–245 (2007).
[2] Topalian, S. L., Drake, C. G., and Pardoll, D. M. *Cur. Opin. Immunol.* **24(2)**, 207–212 (2012).
[3] Parsa, A. T., Waldron, J. S., Panner, A., Crane, C. A., Parney, I. F., Barry, J. J., Cachola, K. E., Murray, J. C., Tihan, T., Jensen, M. C., Mischel, P. S., Stokoe, D., and Pieper, R. O. *Nat. Med.*, **13**, 84–88 (2007).
[4] Alsaab, H. O., Sau, S., Alzrhani, R., Tatiparti, K., Bhise, K., Kashaw, S. K., and Iyer, A. K. *Front Pharmacol.* **6(561)**, 1–15 (2017).
[5] Sasikumar, P. G. N., Ramachandra, M., and Naremaddepalli, S. S. S. *Peptidomimetic compounds as immunomodulators*. WO 2013 0237580 A1, 12 Sep 2013.
[6] Cooper, D. R., Bekah, D., and Nadeau, J. L. *Front. in Chem.*, **2(86)**, 1–13 (2014).
[7] Chithrani, B. D. and Jelveh, S. *Cancers*. **3(1)**, 1081–1110 (2011).

17. An Advanced Multifunctional Hydrogel-Based Dressing for Wound Monitoring and Drug Delivery

Bahram Mirani[1,2,3], Erik Pagan[1,2], Barbara Currie[4], Mohammad Ali Sidduqui[1], Mohsen Akbari[1,2,3]

[1] Laboratory for Innovation in Microengineering (LIME), Department of Mechanical Engineering, University of Victoria, Victoria, BC V8P 5C2, Canada. [2] Center for Biomedical Research (CBR), University of Victoria, Victoria, BC V8P 5C2, Canada. [3] Center for Advanced Materials and Related Technologies (CAMTEC) University of Victoria, Victoria, BC V8P 5C2, Canada. [4] Department of Biochemistry and Microbiology, University of Victoria, Victoria, BC V8P 5C2, Canada.

Abstract

The treatment of epidermal wounds has become a major challenge and has posed a considerable financial burden on the global health care system. Wound healing process can be affected by several factors such as diseases, aging, wound size, and infection. Among these factors, wound infection can lead to delayed wound healing, increased treatment cost, and increased mortality. Therefore, an early diagnosis can play an important role to avoid the medical complications resulted from wound infection. To address this challenge, we have developed a multifunctional wound dressing, made of alginate hydrogel, for early detection and inhibition of bacterial growth in epidermal wounds. For this purpose, pH level of the wound was used as an indicator of bacterial infection and an array of colorimetric pH sensors was embedded in the transparent hydrogel dressing to track the pH level in different regions of the wound. The colorimetric monitoring of pH was implemented through a developed smartphone interface which allows clinicians to track the wound condition in real-time. The capability of the wound dressing to diagnose infection was evaluated *ex vivo* on pig skin sample, infected with *Pseudomonas aeruginosa*, representing the ability of the dressing to detect different densities of the bacterial growth. Furthermore, antibiotic-loaded components were also integrated into the dressing to sustainably release gentamicin sulfate and inhibit bacterial colonization at the wound site. This antibacterial activity was tested *in vitro* on the same strain of bacteria in which the use of 2 mg/ml of gentamicin sulfate led the bacterial eradication.

18. Transport Properties of Metal Nanoparticle-Molecular Electronic Networks

A. Venkataraman, P. Zhang, C. Papadopoulos
Department of Electrical and Computer Engineering, University of Victoria, Victoria, British Columbia, V8W 2Y2, Canada
e-mail: anushav@uvic.ca

The study of electron transport through molecules is an important aspect in realizing the practical application of molecular electronics [1]. Analysis of transport properties of metal-molecular junctions using various state-of-art computational tools allows for realistic evaluation of properties of molecular systems [2, 3].

In the present work, we study the electronic characteristics and charge transport properties of metal nanoparticle-molecular electronic networks composed of interconnected 1,4 benzenedithiol molecules and Au/Al metallic clusters. Our results were based on first principles electronic structure calculations, and semi-empirical approximations. By examining the resulting molecular orbital spatial distribution (Figure 1a), energy gaps and the number of available states at each energy we elucidate the electronic properties of these networks. We also extend our networks by attaching metallic electrodes on either side to study the transmission properties of the resulting network using plane wave density functional theory simulations [4] (Figures 1b, c). Analysis of these results allows new strategies and work towards the development of bigger metal-molecular networks that can be used in building molecular integrated circuits [5] leading to further miniaturization and novel functionality in future electronics.

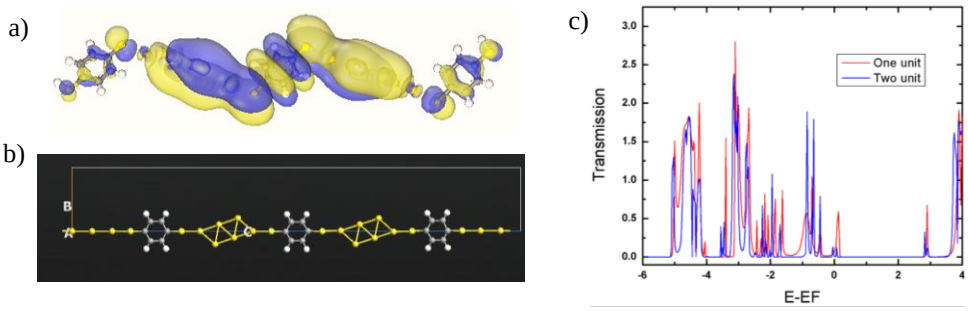

Fig. 1: Au-benzenedithiol linear network structure; a) calculated molecular orbital distribution, b) structures used for electronic transmission and c) transmission vs. energy for different chain lengths.

This work was funded in part by an NSERC Discovery Grant and we acknowledge computational support from WestGrid (www.westgrid.ca) and Compute Canada (www.computecanada.ca).

References

[1] F. Chen and N. Tao, *Accounts of Chemical Research*, **vol. 42**, *(3)*, pp. 429-438 (2009).
[2] P. Zhang and C. Papadopoulos, *IEEE Nanotechnology Materials and Devices Conference* (IEEE, Anchorage, AK, USA), p. 1 (2015).
[3] N. Zimbovskaya and M. Pederson, *Physics Reports*, **vol. 509**, *(1)*, pp. 1-87 (2011).
[4] P. Giannozzi *et al.*, *Journal of Physics: Condensed Matter*, **vol. 21**, *(39)*, pp. 395502 (2009).
[5] P. Zhang, A. Venkataraman and C. Papadopoulos, *Physica Status Solidi (b)*, **vol. 254**, *(9)*, 1700061 (2017).

19. A Novel $BaTi_xZr_{(1-x)}O_3$ Lead-Free Single Crystal by High Temperature Solution Growth method

H.-Y. Wu; Z Liu, Hua Wu and Z.-G. Ye[1] *
4D Labs
Simon Fraser University, Department of Chemistry
e-mail: wuhsinw@sfu.ca

The ferroelectric materials are featured by the spontaneous polarization below the phase transition temperature and switchable polarization under external electric fields, giving rise to a typical polarization-electric field (P-E) hysteresis loop. The phase transformation in the ferroelectric materials can be displayed by the temperature dependence of the dielectric constant, which usually shows a sharp peak at Curie temperature. Many ferroelectric materials that exhibit outstanding piezoelectric and ferroelectric properties have the characteristic perovskite structure, which can be generally described by the chemical formula ABO_3. Based on their promising ferroelectric and dielectric properties, ferroelectric materials have found a wide range of applications from high performance capacitors to random access memory, from microwave devices to piezoelectric transducers, sensors and actuators. The relaxor ferroelectric material exhibits a broad dielectric maximum and a significant frequency dispersion of dielectric permittivity, with the temperature of the dielectric maximum (T_{max}) increasing and its magnitude decreasing with increasing frequency, which can be attributed to the presence of the polar nano-regions. No macroscopic phase transition into ferroelectric phase takes place around T_{max} in relaxor ferroelectrics. The disordered distribution of different ions on the equivalent lattice sites, i.e. compositional disorder or chemical disorder, is the essential structural characteristic of relaxors. Many of the high performance ferroelectric materials, e.g. lead zirconium titanate (PZT), or relaxor-based ferroelectric solid solutions, e. g. $Pb(Mg_{1/3}Nb_{2/3})O_3–PbTiO_3$, are lead containing, which is toxic to environment and human health. It will be interesting to explore the microscopic relaxation mechanisms in different relaxor ferroelectrics and it is also essential to develop suitable lead- free or lead-reduced ferroelectric materials with comparable properties as to replace the current usage on lead. In our work, a novel $BaTi_xZr_{(1-x)}O_3$ (BZT) lead free relaxor ferroelectric single crystal was developed by high temperature solution growth method. This single crystal is 1.54 mm in diameter and its composition is confirmed with XPS to be $BaTi_{(0.725)}Zr_{(0.25)}O_3$. This single crystal possesses the tetragonal structure according to our TOPAS refinements. The composition of this single crystal is fairly closed to the morphotropic phase boundary(MPB). The future study is to modify the growth condition to grow a larger BZT single crystal with the composition on MPB to further study the dielectric, ferroelectric and piezoelectric properties of this lead-free single crystal.

References

[1] Z.-G. Ye, J. Material Science, 41 pp. 31-52 (2007)
[2] B. Wang, J. Appl. Phys. 115, 084104 (2014)
[3] T. Maiti, J. Am. Ceram. Soc., 91[6] pp1769-1780 (2008

20. Direct Detection of Circulating Tumor Cells via Nanoparticle Clustering on the Plasma Membrane

R. G. Sobral-Filho[1], L. Devorkin[2], S. Macpherson[2], A. Jirasek[2], Julian J. Lum[2], A. G. Brolo[1*]
[1]University of Victoria, Department of Chemistry
[2]British Columbia Cancer Agency, Deeley Research Centre
e-mail: agbrolo@uvic.ca, regie@uvic.ca

The promise of nanotechnology has reached prime stances in the last few decades. From the biomedical perspective, therapy and diagnostic are the main branches of interest for nanomaterials. Biological systems are complex and dynamic and many approaches for nanobioanalysis lack the versatility to allow for an effective diagnostic tool. Metallic nanoshells are highly scattering nanoparticles composed of a dielectric core and a thin metallic shell. Control over these two parameters can yield a platform that has been predicted to be suitable for cell analysis, but has not yet been unveiled. We demonstrate the development of the first platform based on the use of finely-tuned nanoshells for the detection of circulating tumor cells (CTCs). With metastasis being the major cause of cancer-related death worldwide, and CTCs are the main effector to that process, it becomes clear the importance of establishing new technologies to detect these cells. Extensive in vitro testing showed the good performance of our platform and in vivo/ex vivo experiments completed the preclinical validation of this detection system. 4T1 mammary carcinoma cells were transfected with a non-native target molecule and tumors were implanted in several mice. Blood was then collected at several post-implantation timepoints and CTC detection was performed with the use of our nanoshell-based platform.

21. 4D LABS – An Open-Access Materials Research Facility

N. Sieb[1]
[1]Simon Fraser University, 4D LABS
e-mail: sieb@4dlabs.ca

4D LABS is an applications- and science-driven materials research facility at Simon Fraser University. We offer access to multiple facilities housing state-of-the-art equipment for academic, industrial and government researchers. We focus on accelerating the Design, Development, Demonstration and Delivery of advanced functional materials and nanoscale devices. Our goal-oriented environment fosters intellectual freedom and creativity—critical for breakthrough research.

The Fabrication and Prototyping Facility offers micro- and nanofabrication equipment and associated tooling for developing new prototypes with novel materials. Much of this equipment is located in our class 100 Clean Room. The Materials and Device Testing Facility provides access to instrumentation for the high resolution characterization of novel materials and new devices. These tools enable researchers to complete in-depth investigations of material properties, including microstructure, defects, composition, and crystallinity.

We provide training and support from our experienced staff of scientists and engineers who maintain the diverse set of equipment and processes to meet your needs in lithography, thin film growth and deposition, and materials and process characterization. We provide hands-on, one-on-one training in the operation of the instruments and mastery of techniques. We strive to provide our users access to the equipment and expertise necessary for success in their research and development projects. We encourage you to contact us to discuss how we can be of assistance to you.

This work made use of the 4D LABS shared facilities supported by the Canada Foundation for Innovation (CFI), British Columbia Knowledge Development Fund (BCKDF), Western Economic Diversification Canada (WD), and Simon Fraser University (SFU).

22. Effect of oxidation on the optical properties of Zn_3N_2 powders

Helaleh Alimohammadi, Thomas Tiedje, Peng Wu

[1] Department of Electrical and Computer Engineering, University of Victoria, Victoria, British Colombia, Canada

e-mail: halimohangar@email.com

Zinc nitride is currently attracting research interest because of its potential for novel electronic and photonic properties. In this thesis the optical properties of Zn_3N_2 powders have been investigated by photoluminescence (PL) and diffuse reflectance spectroscopy (DR) measurements. The micro structure and composition of zinc nitride were assessed by scanning electron microscopy (SEM) and powder X-ray diffraction (PXRD). Measurements of PL, PXRD and DR were carried out on zinc nitride powder samples with different oxygen-nitrogen (O/N) ratios. Photoluminescence spectroscopy of the zinc nitride powder samples allows us to find the optical bandgap of the samples. To the best of our knowledge, this is the first report on the low temperature photoluminescence of zinc nitride powder. This showed us how the band gap energy depends on temperature. The diffuse reflectance measurement let us determine a direct bandgap of 1.12eV for Zn_3N_2 powders and the PL measurements also demonstrated emission at the same photon energy. In this work, the effect of oxidation on the optical properties has been investigated. The surface oxidation of Zn_3N_2 powders and the oxygen-nitrogen (O/N) ratio were detected through PXRD scans. Our measurement show that the optical bandgap energy shifts to lower energy due to the oxygen incorporation. The reduction of the Zn_3N_2 bandgap by oxygen incorporation can be explained by a resonant interaction between the extended states of the conduction band of Zn_3N_2 and localized oxygen states near the conduction band edge. Additionally, the thermal nitriding process was carried out on the oxidized Zn_3N_2 powders to vary the O/N ratio which increased the bandgap energy. From our result, the optical bandgap of the Zn_3N_2 powders is estimated to be ~1.2 eV which decreases by small amount of oxygen contamination due to exposure to air. Powder XRD measurements of thermal oxidation of Zn_3N_2 indicated that the oxidation of these powders is slow at room temperature.

23. Long-Life Operation of Flexible Ionic Devices Using Spray-Coated Elastomeric Encapsulation

Saeedeh Ebrahimi Takalloo[1], Katelyn Dixon[1], Adelyne Fannir[2], Cedric Plesse[2], Giao T.M Nguyen[2], Frederic Vidal[2], John D. W. Madden[1]

Electrical and Computer Engineering, University of British Columbia, Vancouver, BC, Canada[1]

Laboratoire de Physicochimie des Polymères et des Interfaces, Université de Cergy-Pontoise, Cergy, France[2]

Email: saeedebr@ece.ubc.ca

Ionic electroactive polymers such as conducting polymers, ionic polymer metal composites (IPMC) and hydrogels have attracted attentions in recent decades due to their mechanical flexibility, light weight and easy manufacturing. They have been widely used as actuators, sensors and energy harvesters. Despite the difference in their structures and mechanism of operation involved, they all require an electrolyte containing enough ions to operate. Electrolyte is mainly a solution of a salt into a polar solvent such as water or a less volatile solvents such as propylene carbonate (PC) or acetonitrile (ACN). This suggests that the performance of ionic devices degrades over time as the solvent evaporates from the device.

In this work, PEDOT trilayer conducting polymer actuators are encapsulated with the commercial grade styrene-b-isobutylene-b-styrene (SIBSTAR®), a thermoplastic elastomer which has already been shown to be a proper candidate as an encapsulating material for trilayer conducting polymer actuators. SIBSTAR® exhibits small elastic modulus of < 10 MPa (The elastic modulus of CP trilayers is ranging between 200-500 MPa) and large elongation at break of 600 % making it suitable as the outer encapsulating shield.

Six samples of PEDOT/ PEO: NBR/ PEODT trilayer actuators were prepared and immersed into a 1M solution of LiTFSI in PC for over a month. (dimensions: 5mm ×15mm ×0.360 mm) Spray coating of SIBSTAR solution (2 % in Toluene) was done using a Sono-Tek spray coater. Each three samples were spray coated with 45 µm, 90 µm and 180 µm thick SIBSTAR. The samples were then stored in a room with controlled temperature of 23±1˚C and relative humidity of 50 ± 2 %. The mass of samples was measured over time using a precision scale. Three other trilayer samples of the same dimensions with no encapsulation were also stored the same way as the encapsulated samples to monitor the mass loss of PC when there is no encapsulation.

Results shows that a trilayer with the dimensions mentioned above has an average total PC mass of 14.5±1 mg which evaporates exponentially over time. It takes 15 hours to lose 25% of the PC content stored into the trilayer with no encapsulation. This is while for encapsulated trilayers with 45 µm and 90 µm thick films of SIBS, the device needs more than 200 and 500 days to lose 25% of its solvent content respectively. Force and deflection angle measurements shows that encapsulation does not have a significant effect on the force generated while the deflection angle decreases as encapsulation is applied and decreases more as the thickness of encapsulation increases.

Acknowledgement: This work made use of the 4D LABS shared facilities supported by the Canada Foundation for Innovation (CFI), British Columbia Knowledge Development Fund (BCKDF), Western Economic Diversification Canada (WD), and Simon Fraser University (SFU).

References:

[1] S. Naficy, N. Stoboi, P.G. Whitten, G.M. Spinks, G.G. Wallace., *Smart materials and structures*. **22(7)**, 075005 (2013).

24. Solvent Isotope Effect on Biomolecular Adsorption at Hydrophobic Surfaces

Tasha A. Jarisz[1], Kailash C. Jena[1], Matthew C. Dixon[2], Dennis K. Hore[1*]

[1]Department of Chemistry, University of Victoria, Victoria BC, Canada, V8W 3V6
[2]Biolin Scientific Inc., 215 College Road, Paramus NJ, 07652
[*]dkhore@uvic.ca

A more complete understanding of the interactions of biomolecules with hydrophobic surfaces is integral to enhanced biocompatibility of materials used in a variety of biomedical applications [1-3]. In vibrational spectroscopic studies of biological systems, oftentimes D_2O is substituted for H_2O in order to more clearly resolve the amide I and C-H stretching regions. This is especially important in protein studies, where water bending modes can interfere in these regions. Studies have shown that small changes in the solvent structure have significant effects on protein stability, folding, and structure [4]. Consequently, in interfacial studies where adsorption is involved, the interchangeability of H_2O and D_2O may not be straightforward, as the two solvents may have a significant impact on the amount adsorbed and/or the adsorbed structure.

One of the challenges associated with studying adsorption at solid-liquid interfaces is achieving sufficient surface specificity in the presence of bulk solution. Nonlinear vibrational sum frequency generation (SFG) spectroscopy has proven an ideal technique for studying the interfacial structure of biomolecules. This is because the second order nonlinear susceptibility is non-zero only at the surface where the symmetry is broken. Here, SFG is used to study the adsorption of the amino acid leucine onto a polystyrene surface from H_2O and D_2O. SFG spectra show remarkable differences in the alkyl stretching region, with modes being much more pronounced for leucine in D_2O than in H_2O.

A quartz crystal microbalance with dissipation monitoring (QCM-D) is also used to study the amount of leucine adsorbed onto polystyrene sensors in both H_2O and D_2O. Analysis of the data using a Voigt model led to the conclusion that more than twice as much leucine adsorbed onto the surface when D_2O was used as the solvent. When this ratio of adsorbed surface mass in D_2O versus H_2O is used to model the second-order nonlinear response, both the intensity and the overall appearance of the SFG spectral features are entirely accounted for. This means that the marked spectral differences in the two solvent environments are a result of changes in the population of leucine at the surface, and not a result of changes in its adsorbed structure. This highlights the importance of solvent in biomolecular adsorption at hydrophobic surfaces, and its role in dictating the amount adsorbed, while not altering the structure after adsorption.

This work was supported by a Discovery Grant from the National Science and Engineering Research Council of Canada (NSERC) and Biolin Scientific.

[1] Kasemo, B. Curr. Opin. *Solid State Mater. Sci*., ***3***, 451-459 (1998).
[2] Lu, J. R.; Zhao, X.; Yaseen, M. *Curr. Opin. Coll. Inter.*, ***12***, 9-16 (2007).
[3] Miyata, T; Uragami, T.; Nakamae, K. *Adv. Drug Delivery Rev*., ***54***, 79-98 (2002).
[4] Efimova, Y. M.; Haemers, S.; Wierczinski, B.; Norde, W.; van Well, A. *Biopolymers*., ***85***, 264-273 (2006).

25. Detection of Electrooxidation Products in Microfluidic Devices Using Raman Spectroscopy

T. Li[1,2], T. Holm[1,2], D.A. Harrington[1,2*]
[1]Centre for Advanced Materials and Related Technologies
[2]University of Victoria, Department of Chemistry
e-mail: dharr@uvic.ca

Microfluidics combining with Raman Spectroscopy has great promise for monitoring reaction process with very little volume of liquid provided. This advanced method for in-situ and online detection allows for flexible manipulation of fluids, micro/nano-particles, and biological samples[1]. Microfluidic methods reduce the sample volume as well as improve the accuracy of monitoring, and Raman Spectroscopy allows semi-quantitive analysis, which is very promising for identifying and quantifying the products of alcohol electrooxidation.

This research makes use of a channel where the laser focuses at or near a Pt wire/mesh working. The channel is connected to a downstream reservoir with a reference electrode and counter electrode. A Teflon tube connected to a pump flows the liquid through the channel at a pre-set flow rate to oxidize alcohol for downstream/on-wire measurements. Highly concentrated KOH (5 M) is used as the electrolyte, and 5 M methanol is used to ensure a high S/N ratio in the Raman spectra.

A time sequence of spectra taken with the laser focused on the Pt WE show production of formate (the main product), and its dependence on time, potential, flow rate and laser position were investigated.

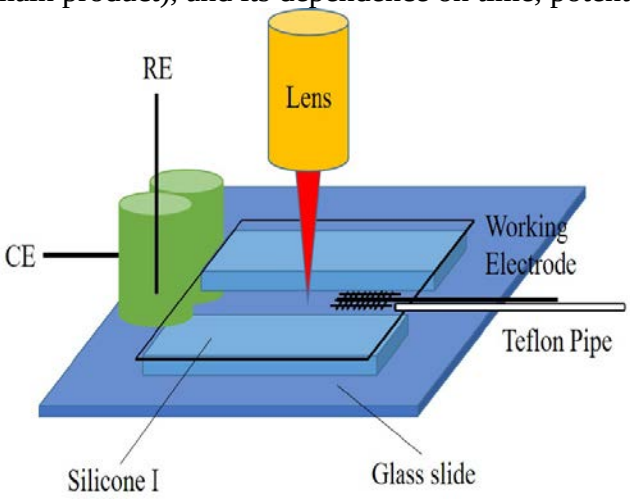

Figure 1 Cell Design

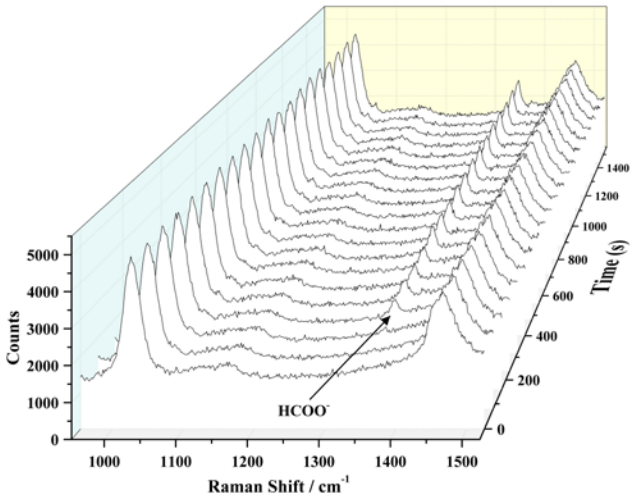

Figure 2 Time-dependent Raman Spectra

This research was conducted as part of the Engineered Nickel Catalysts for Electrochemical Clean Energy project administered from Queen's University and supported by Grant No. RGPNM 477963-2015 under the Natural Sciences and Engineering Research Council of Canada (NSERC) Discovery Frontiers Program.

References

[1] A.F. Chrimes, K. Khoshmanesh, and K. Kalantar-zadeh, *Chem. Soc. Rev.*, **42**, 5880 (2013).

26. Synthesis and Characterization of New Au- and Ag-Based Plasmonic Alloy Materials

Yuan, Xiaoyun (Kelsy)[1]; Sasan V. Grayli[1]; Gary W. Leach[1].
[1] Simon Fraser University, Department of Chemistry, xiaoyuny@sfu.ca.

Confining the delocalized fields of electromagnetic waves to the nano-scale of metallic surface regions by exciting surface plasmons enables new methods of information transfer, energy conversion, red-ox chemistry and catalysis. Currently, Ag and Au are the most commonly used plasmonic materials, but neither is ideal. [1]

Our goal is to synthesize and characterize new Au- and Ag-based plasmonic alloy materials with improved plasmonic response, low optical losses and high chemical stability by employing an electroless reduction method to deposit the alloys through co-deposition of silver and gold ions. We have examined the deposition kinetics of the ions in solution, and characterized the resulting films. We have analyzed their optical and plasmonic properties using spectroscopic ellipsometry, their composition using X-ray Photoelectron Spectroscopy (XPS), and their crystalline structure and morphology using X-ray Diffraction (XRD) and scanning electron microscopy (SEM). The chemical stabilities of the alloy films have also been addressed by examining their stability upon exposure to peroxide.

The development of new, high quality, crystalline, plasmonic alloy materials will enable improved performance in plasmonic and metamaterial research and application.

This work was supported by CMC and 4dlabs.

References

[1] Murray, W. Andrew, and William L. Barnes. "Plasmonic materials." *Advanced materials*, **19**, no. 22 (2007): 3771-3782.

27. Growth and Characterization of $PbHfO_3$-$Pb(Mg_{0.5}W_{0.5})O_3$ Antiferroelectric Single Crystals by Flux Method

P. Gao[1,2], N. Zhang[1], H. Wu[1,2], A.A. Bokov[1], and Z.-G. Ye[1,2,*]

[1]Simon Fraser University, Department of Chemistry and 4D LABS
[2]Xi'an Jiaotong University, Department of Electronic and Information Engineering
[3]Donghua University, Department of Applied Physics
e-mail: Pan_Gao@sfu.ca

A new solid solution of complex perovskite structure, $0.99PbHfO_3$-$0.01Pb(Mg_{0.5}W_{0.5})O_3$ antiferroelectric single crystal, have been successfully grown by the high-temperature solution growth method and the top-cooled solution growth method. The chemical and thermodynamic parameters, including the flux concentration, the soaking temperature and the cooling rate, have been optimized. The as-grown single crystals display brown color with size of 1-2 mm. Its crystal structure, dielectric, optical and antiferroelectric properties are investigated. The single crystals show two dielectricpeaks at 138°C and 189°C, corresponding to antiferroelectric-ferroelectric and ferroelectric-paraelectric phase transitions. The softening of antiferroelectric order and the improvement in induced polarization make the PHf-PMW single crystal an interesting material system for such applications as energy storage devices.

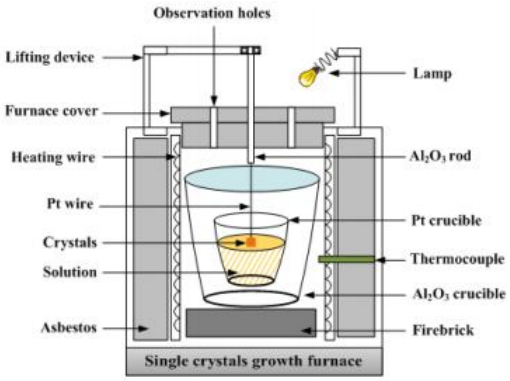

Fig.1. Furnace and crucible set-up for HTSG and TCSG

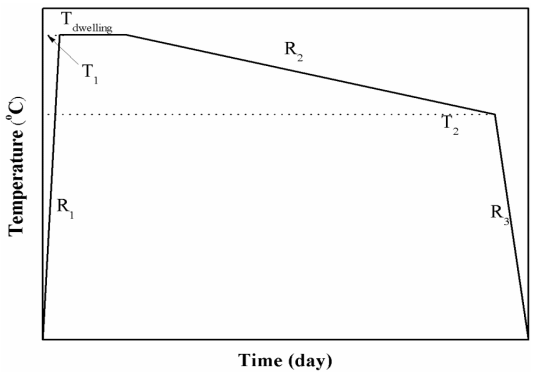

Fig.2. Typical temperature profile for the crystal growth

This work was supported by the U. S. Office of Naval Research (Grants No.N00014-12-1-1045 and N00014-16-1-3106), the Natural Sciences and Engineering Research Council of Canada (NSERC, Grant No. 203773), the Natural Science Foundation of China (Grant No. 51602243), the "111 Project" of China (Grant No. 2010*ZGY and WR also acknowledge the "Qianren Program" of the Chinese Government for support.*

References

[1] C. Liu, F. Li, and H.-M. Cheng, Adv. Mater., 22, E28-E62 (2010).
[2] A.K. Tagantsev, K. Vaideeswaran, and N. Setter, Nat. Commun., DOI: 10.1038/ncomms3229.
[3] X.H. Hao, J.W. Zhai and Z.K. Xu, Prog. Mater Sci., 63, 1-57 (2014).

28. An Electroless Approach to Fabricate High Efficiency Plasmonic Gold Nano-Antennas

S. V. Grayli[1], S. Kamal[2], X. Zhang[3], G. Leach[4]

[1]PhD student at Department of Chemistry, Laboratory for Advanced Spectroscopy and Imaging Research, [2] LASIR facility manager,[3]4D LABS staff scientist,[4]Associate Professor at Department of Chemistry, Simon Fraser University

e-mail: sasanv@sfu.ca

Material quality and crystallinity are expected to play an important role in the activity of plasmonic nano-antennas. Plasmonic devices made from monocrystalline metals are expected to display much higher efficiency and stability than polycrystalline devices which are subject to many losses due to the presence of grain boundaries. It has previously been demonstrated by our group that through novel electroless deposition chemistry ultra-smooth gold (Au) films can be grown on single crystal silver (Ag) surfaces. In this approach, the electrochemical incompatibility of Au and Ag can be overcome by decreasing the reduction potential of Au cations in the deposition bath and as a result, ultra-smooth monocrystalline Au films are grown with the same crystalline orientation as the underlying Ag film. Here, we investigate the activity of bowtie nano-antennas fabricated by focused ion-beam (FIB) milling of monocrystalline and polycrystalline Au films. These studies provide a direct measure of plasmonic nanoantenna activity and stability and their dependence on metal quality. The activity of the nano-antennas made on an ultra-smooth Au film was compared to bowtie nano-antennas made on a multi-crystalline Au film.

29. Synthesis and characterization of methyl ester functionalized poly(dicyclopentadiene)

Tong Li, Tyler Cuthbert, Jeremy Wulff *
University of Victoria, Department of Chemistry
e-mail: wulff@uvic.ca

Poly(dicyclopentadiene) (PDCPD) is a thermoset polymer and has been studied for several years. Our research is based on modifying PDCPD with a methyl ester group. After functionalizing cyclopentadiene monomer, we synthesized fPDCPD (Fig. 1A) by ring opening metathesis polymerization (ROMP) with Grubbs' second generation catalyst (G II).

fPDCPD undergoes crosslinking (Fig. 1C) naturally when it is exposed to air once it's been made. The speed of crosslinking increases as temperature increases. To figure out the mechanism of crosslinking, we made both protonated and deuterated linear fPDCPD and then annealed samples under various temperatures for 24 hours or different time points at 135°C. ATR FT-IR, Raman and Solid State NMR spectroscopy were used as characterization techniques. Two selected spectra (Fig. 2A and 2B) showed the changing of fPDCPD through different annealing conditions. From there, we proposed the mechanism of crosslinking of fPDCPD.

Another direction of this project is to synthesize and characterize fPDCPD-based random copolymers (Fig. 1B) with four different monomer mole fractions between fDCPD and DCPD. The SS/NMR spectrum (Fig. 2C) indicates that as we increasing the mole fractions of fDCPD, stronger signals of methyl ester groups have been observed.

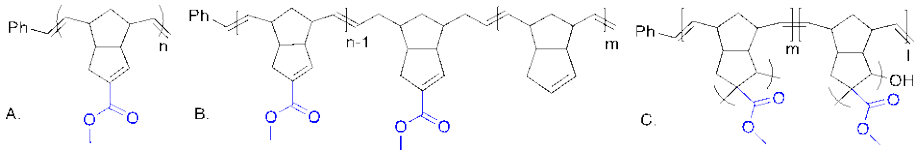

Fig. 1. Chemical structure of: A) linear fPDCPD; B) linear fPDCPD-co-PDCPD; C) cross-linked fPDCPD

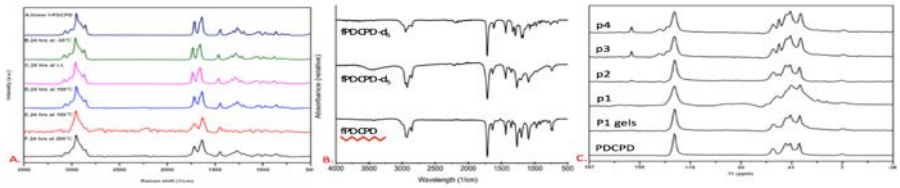

Fig. 2. A) Raman Spectrum of fPDCPD under various temperature annealing conditions for 24 hours; B) FT-IR Spectrum of protonated and deuterated linear fPDCPD; C) Solid State NMR spectrum of random copolymers.

Acknowledgement: Special thanks to Dr. Alexandre G. Brolo, Dr. Stanislav Konorov, Dr. Chris Barr, Alex Wlasenko and Tianyu Li for spectroscopy analysis at Department of Chemistry in University of Vcitoria. Dr. Mathew Willans for running Solid State NMR at The University of Western Ontario. Lastly, Wulff group members for their mental support. This work was supported by NSERC and ACS PRF (American Chemical Society Petroleum Research Fund).

References

[1] J. Chen, F. P. Burns, M. G. Moffitt and J. E. Wulff, *ACS Omega*, **1**, 532-540 (2016)

30. Determining the Orientation of Chemical Functional Groups on Metal Surfaces by a Combination of Homodyne and Heterodyne Nonlinear Vibrational Spectroscopy

W. C. Yang[1], D. K. Hore[1,*],
[1]University of Victoria, Department of Chemistry
e-mail: dkhore@uvic.ca

In this work, we present a scheme to study chemical functional groups on metal surfaces using a combination of homodyne and heterodyne sum-frequency generation spectroscopy (SFG). Unlike dielectric materials, metal surfaces have significant electronic contribution to the second-order signal. As a consequence, traditional heterodyne schemes are inapplicable at this interface due to observed phase degradation from both non-resonant contribution and neighboring mode effects. Here we illustrate how we can overcome this challenge by combining metal phase information from the heterodyne experiment with homodyne spectra in both experimental and simulated data. Furthermore, we also propose a model to predict the observed phase change in the heterodyne scheme.

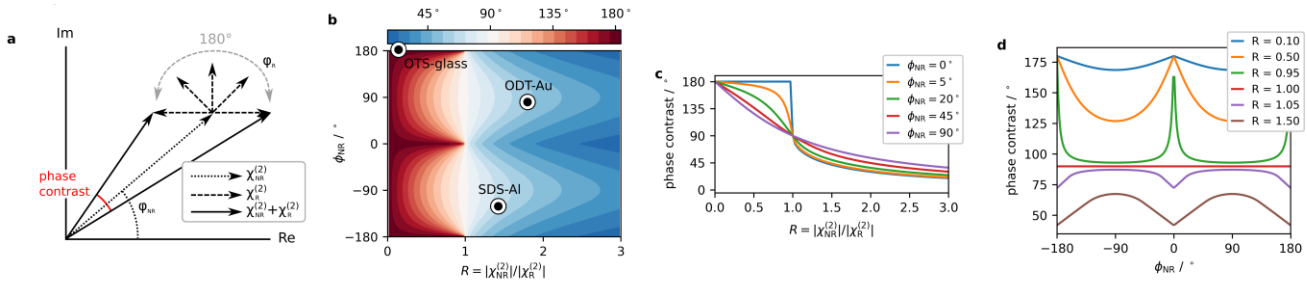

Fig. 1(a) illustrates the determination of the phase contrast in the complex plane, and (b) shows its predicted phase contrast as a function of the non-resonant to resonant amplitude ratio and the phase of the non-resonant. (c) shows slices along the non-resonant phase direction and (d) shows some slices along the ratio direction.

We have examined our model with four different experimental cases to demonstrate the predictability of the simulation with aluminum, OTS-glass, SDS-aluminum, and ODT-gold. As well, we illustrate some limiting and special cases with respect to the non-resonant phase and amplitude ratio. Finally, we have concluded some general rules regarding the orientation of the methyl and free OH functional groups with respect to the amplitude, non-resonant phase as well as the polarity parameter, $P = \mathrm{sgn}(A \cdot \sin\varphi_{NR})$, where A is the amplitude and $\sin\varphi_{NR}$ is the non-resonant phase.

This work was supported by the Natural Sciences and Engineering Research Council of Canada (NSERC) with a Discovery Grant, Imperial Oil for a University Research Award, and a Collaborative Research and Development grant from NSERC in partnership with Imperial Oil.

31. Visualising the effect of cucurbit[6]uril on the structure of sodium deoxycholate gel using fluorescence microscopy

Sree Gayathri Talluri[1], M. Seyedalikhani[1] and C. Bohne[1*]

[1]University of Victoria, Department of Chemistry
e-mail: sreegayathri1994@gmail.com

Supramolecular gels are self-assemblies formed mainly by non-covalent interactions such as hydrogen bonding, electrostatic interactions, π-π stacking and hydrophobic forces. Sodium deoxycholate (NaDC) is a bile salt, known for its ability to form a supramolecular gel within a certain pH range[1]. These gels are biocompatible and reversible, which makes them interesting to explore from a drug delivery point of view. However, the low mechanical strength of NaDC gels results in premature dissolution of the gel, which limits their use in drug delivery applications.

The objective of the present work was to investigate the effect of CB[6] on the mechanical strength of NaDC gels and to study how this in-turn affects the gel's structure at the microscopic level. Mechanical strength of the gels was measured using vial inversion tests, where the time required for the gel to fall under gravity was recorded at a constant temperature. These measurements are complemented with rheology studies. Structural characterisation was done using fluorescence microscopy, where the gel network was tagged with positively charged dyes such as rhodamine 6G or acridine orange by means of electrostatic interactions. Changes in the gel's structure were studied at different length scales in the presence of CB[6].

Initial structural studies on NaDC gel network resulted in undefined features. On addition of CB[6], the network showed more defined features of size around 5 μm. However, these results are non-conclusive at this point. Therefore, we decided to use a supramolecular gel that was imaged previously as a model to develop the required methodology. Chitosan is a supramolecular gel, whose structure has been studied using fluorescence microscopy[2]. For the chitosan gel (Fig. 1) we observed features similar to those reported and we are using this gel to optimise the experimental setup.

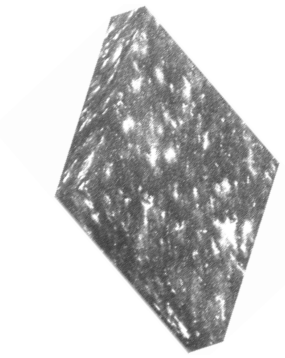

Figure 1: Microstructural 3D reconstruction image of chitosan (1% w/v) gel tagged with FITC (9 μM) from LSCM. Scale bar = 10 μm.

References:

1. Valenta, C.; Nowack, E.; Bernkop-Schnürch, A. *International Journal of Pharmaceutics* **1999**, *185*, 103.
2. Crompton, K.E.; Prankerd, R.J.; Paganin, D.M.; Scott, T.F.; Horne, M.K.; Finkelstein, D.I.; Gross, K.A.; Forsythe, J.S. *Biophysical Chemistry* **2005**, 117, 47-53.

32. Synthesis, Structure and Electrical Properties of A Novel Piezo- /Ferroelectric Solid Solution: (1-*x*)$PbTiO_3$ - *x*$Bi(Zn_{2/3}Ta_{1/3})O_3$

Yuan, Yi[1]; Z. -H, Liu[1,2]; M, Bari[1]; H, Wu,[1,3]; Z. -G, Ye[1*]

[1]Department of Chemistry and 4D LABS, Simon Fraser University, Burnaby, British Columbia, V5A 1S6, Canada

[2]Electronic Materials Research, Key Laboratory of the Ministry of Education & International Center for Dielectric Research, Xi'an Jiaotong University, Xi'an, 710049, China

[3]Department of Applied Physics, Donghua University, Ren Min Road 2999, Songjiang, Shanghai, 201620, China

e-mail: yya155@sfu.ca

Piezo-/ferroelectric materials, which can function at high temperatures and electric fields, are highly desired for transducers, sensors and actuators. These applications of current high-performance lead-based materials are greatly limited due to their relatively low Curie temperatures (T_C <*200°C*) and coercive fields (E_C <5kV/cm). Additionally, their high lead contents present a big concern about lead toxicity to human health and environment. In this work, a novel lead-reduced binary solid solution system *x*$Bi(Zn_{2/3}Ta_{1/3})O_3$-(1-*x*)$PbTiO_3$ (*x*=0 *to* 1) was synthesized by solid state reaction method and the crystal structure and electrical properties were systematically investigated using various techniques. A formation of solid solution from *x*=0 to 0.27 with tetragonal phase symmetry of perovskite structure was found by means of powder X-ray diffraction. Ultrahigh tetragonality (*a/c*>1.06) was observed in this system indicating large crystal distortion and polarization. Dielectric measurements were performed and confirmed high Curie temperatures (*>450°C*). Ferroelectric characterization showed a potential high coercive field (E_C > 20kV/cm) in this system. The origin of these electrical behaviors were explained from the crystal chemistry aspect[1-3]. The high-T_C and high-E_C features signify that the $Bi(Zn_{2/3}Ta_{1/3})O_3$-$PbTiO_3$ system is a promising and more environmental friendly candidate for electromechanical transduction applications that can operate in a wider temperature and electric field range.

References

[1] I, Grinberg *et al*. *Phys. Rev. B.* **98**, 10760 (2007).
[2] I, Grinberg *et al*. *Phys. Rev. B.* **70**, 220101(2004).
[3] M. R, Suchomel *et al*. *Appl Phys Lett.* **86**, 262905(2005).

33. Nano-Micro Fabrication Technique for Large-Area High-Performance Solar Cells, Displays and Biosensor Arrays

Authors: Sahar Sam[1,2], Weng Fan[1,2], Jehad Alsaif[1,2], Amin Ebrahimi[1,2], Manyan (Amy) Xu[1,2], Aaron Mueller[1,3], Vinayak Pendharkar[1] and Rustom Bhiladvala[1,2]

[1]Nanoscale Transport, Mechanics and Materials Laboratory, Departments of Mechanical Engineering, University of Victoria, Victoria, BC, Canada.

[2]CAMTEC, Centre for Advanced Materials and Related Technologies, University of Victoria, Victoria, BC, Canada.

The remarkable mechanical, optical, thermal and electronic properties of one-dimensional structures such as nanowires (NWs) have enabled the construction of devices with extraordinary capabilities. Their landmark demonstrations in publications from research laboratories are limited to a small number of devices due to high fabrication cost. We have developed a low-cost technique to fabricate a diversity of large-area high-performance devices such as biosensor arrays and transparent electrodes. Our recent analytical work has enabled quantitative guidelines to choose the best parameter values to maximize device yield and enhance performance. Using these guidelines, the parameter values can now be chosen without a set of time-consuming and expensive trial-and-error steps, that have been a barrier to its use. Following the guidelines, we have demonstrated high yield of mechanical nanoresonators, which can serve as specific biomolecule sensors, and of high performance transparent electrodes, a crucial component of devices such as displays and solar cells.

This work was financially supported by Canadian agencies NSERC, CFI, BCKDF and MITACS and made use of the 4D LABS at Simon Fraser University.

References

[1] Z. Liu et al., Chemical Society Reviews, 44, 161-192 (2015)
[2] M. Sam et al., Nanoscale 8, 889-900 (2016)
[3] M. Sam et al., Materials Letters163, 205-208 (2016)
[4] N. Moghimian., Electrochimica Acta 114, 643-648 (2013)
[5] N. Moghimian., Materials Letters 113, 152-155 (2013)
[6] R.B. Bhiladvala et al., Nature Nanotechnology 3, 88-92 (2008)
[7] M. Sam, P.hD. Dissertation, University of Victoria (2016)

34. Analysis of Egg White Protein Composition with Double Nanohole Optical Tweezers

Noa Hacohen, Candice J. X. Ip, and Reuven Gordon*
University of Victoria, Department of Electrical and Computer Engineering
e-mail: rgordon@uvic.ca

We use a double nanohole optical tweezer to analyze the protein composition of egg white through analysis of many individual protein trapping events. The proteins are grouped by mass based on two metrics: standard deviation of the trapping laser intensity fluctuations from the protein diffusion, and the time constant of these fluctuations coming from the autocorrelation. Quantitative analysis is demonstrated for artificial samples, and then the approach is applied to real egg white. The composition found from real egg white corresponds well to past reports using gel electrophoresis. This approach differs from past works by allowing for individual protein analysis in heterogeneous solutions without the need for denaturing, labelling or tethering.

35. Growth of h-BN on copper (110) in a LEEM

C. Herrmann*, P. Omelchenko, K.L. Kavanagh
Simon Fraser University, Department of Physics
*e-mail: cherrman@sfu.ca

Hexagonal boron nitride (h-BN) was grown by borazine vapour deposition on single crystalline Cu (110) substrates at 740°C. The growth was investigated in situ using a Low-Energy Electron Microscope (LEEM). Substrates were prepared ex situ by mechanical and electrochemical methods and once in the LEEM system, by annealing in a H2 atmosphere resulting in a reconstructed surface. Exposure to borazine vapour resulted in the nucleation of well-aligned trigonal h-BN islands, which merged to ribbons along surface steps, and into larger, more irregularly shaped features. A coverage of up to 60% was achieved with an exposure of 3900 L. A diffraction ring in the low energy electron diffraction pattern was observed with a preferential alignment along the Cu ⟨ 111⟩ directions of the underlying substrate. Low-energy electron reflectivity scans, as well as x-ray photoelectron and Raman spectroscopies, confirmed the presence of a partial monolayer of h-BN on the surface. [1]

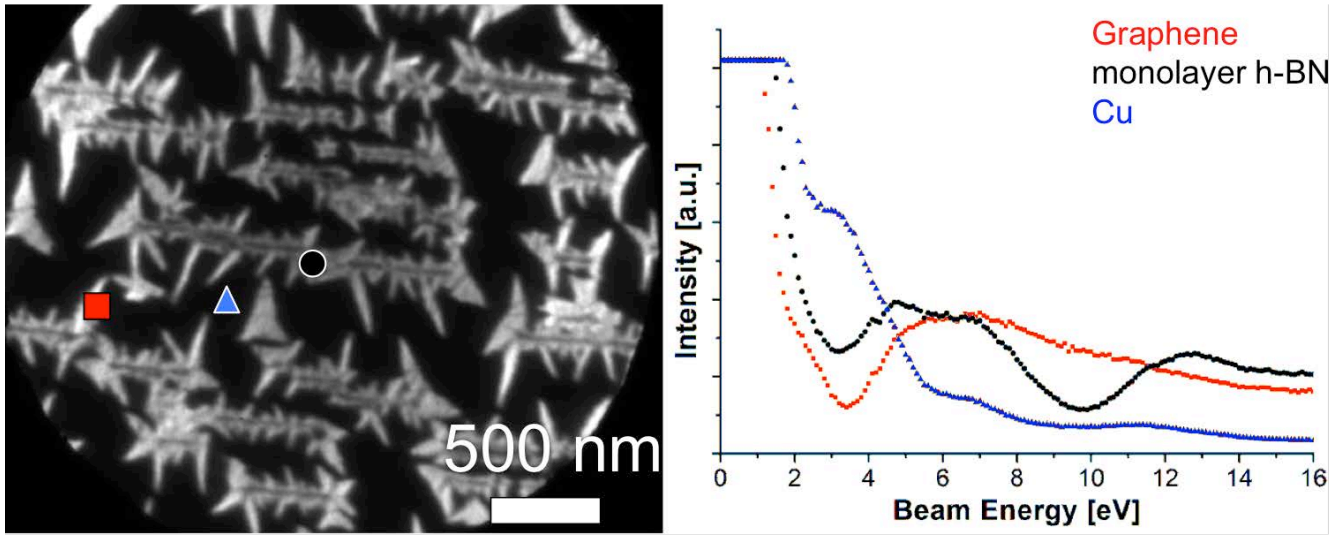

Fig. 1 (left) LEEM BF image of a borazine exposed Cu (110) sample showing bright regions of h-BN. **(right)** LEER spectra of positions indicated in the left image, showing different behavior for h-BN (black) and graphene (red) regions.

We are grateful for funding support from NSERC, CFI/BCKDF, and SFU 4D-Labs.

References

[1] C. Herrmann, P. Omelchenko, K.L. Kavanagh, *Surface Science*, (2017), 10.1016/j.susc.2017.11.021